10-2011

All-Spin Logic Device With Inbuilt Nonreciprocity

Srikant Srinivasan
Purdue University, srikant@purdue.edu

Angik Sarkar
Purdue University, sarkara@purdue.edu

Behtash Behin-Aein
Purdue University, behinb@purdue.edu

Supriyo Datta
Purdue University, datta@purdue.edu

Srinivasan, Srikant; Sarkar, Angik; Behin-Aein, Behtash; and Datta, Supriyo, "All-Spin Logic Device With Inbuilt Nonreciprocity" (2011). *Birck and NCN Publications.* Paper 847.
http://dx.doi.org/10.1109/TMAG.2011.2159106

All-Spin Logic Device With Inbuilt Nonreciprocity

Srikant Srinivasan[1,2], Angik Sarkar[1,2], Behtash Behin-Aein[1,2], and Supriyo Datta[1,2], *Fellow, IEEE*

[1]School of Electrical and Computer Engineering, Purdue University, West Lafayette, IN 47907 USA
[2]NSF Network for Computational Nanotechnology (NCN), West Lafayette, IN 47907 USA

The need for low-power alternatives to digital electronic circuits has led to increasing interest in logic devices where information is stored in nanomagnets. This includes both nanomagnetic logic, where information is communicated through magnetic fields of nanomagnets, and all-spin logic (ASL), where information is communicated through spin currents. A key feature needed for logic implementation is nonreciprocity, whereby the output is switched according to the input but not the other way around, thus providing directed information transfer. The objective of this paper is to draw attention to possible ASL-based schemes that utilize the physics of spin-torque to build in nonreciprocity, as in transistors, that could allow logic implementation without the need for special clocking schemes. We use an experimentally benchmarked coupled spin-transport/magnetization-dynamics model to show that a suitably engineered single ASL unit indeed switches in a nonreciprocal manner. We then present heuristic arguments explaining the origin of this directed information transfer. Finally, we present simulations showing that individual ASL devices can be cascaded to construct a ring oscillator circuit, which provides a clear signature of inbuilt directionality.

***Index Terms*—All-spin logic, magnetization dynamics, ring oscillator, spin circuits, spin transfer torques, spin transport, spintronic logic devices, unidirectional network.**

I. Introduction

DIGITAL electronic circuits store information in the form of capacitor charges that are manipulated using transistor-based switches. The need to find low-power [1] alternatives has led to increasing interest in alternative schemes that store information in nanomagnets. This includes both nanomagnetic logic (NML) [2], [3] where the magnets communicate through their magnetic fields and all-spin logic (ASL) [4], [9] where communication is through spin currents.

A key feature needed for logic implementation is nonreciprocity, whereby the output is switched according to the input but not the other way around. In NML, this nonreciprocity has been achieved through Bennett clocking [2], [3], [5], [6], which requires additional clocking circuitry as compared to standard transistor-based logic. The objective of this paper is to draw attention to possible ASL-based schemes that utilize the established physics of spin-torque to provide an inbuilt nonreciprocity similar to transistors, thereby allowing logic implementation without the need for special clocking schemes.

A. ASL Design and Operation

First, let us state clearly the operation of the proposed device and how introducing nonreciprocity can make it function in a deterministic manner. A generic ASL device is shown in Fig. 1(a), consisting of identical input (FM_1) and output (FM_2) ferromagnets connected to a common voltage source V_{SS} that drives a charge current across the ferromagnets to a ground contact through a common nonmagnetic channel. Although both magnets are connected to the same voltage, significant spin current ($\vec{I}_S$) is exchanged between them as will be shown in subsequent sections.

Manuscript received February 21, 2011; accepted May 25, 2011. Date of current version September 23, 2011. Corresponding author: S. Datta (e-mail: datta@purdue.edu).

Color versions of one or more of the figures in this paper are available online at http://ieeexplore.ieee.org.

Digital Object Identifier 10.1109/TMAG.2011.2159106

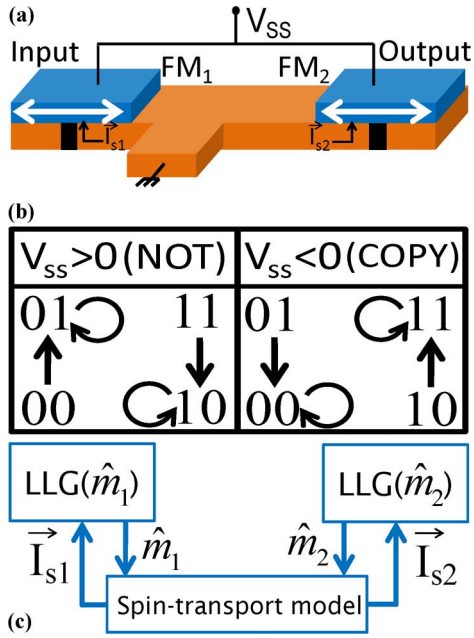

Fig. 1. Basic operation of a generic ASL device. (a) Suggested layout showing two identical Ferromagnets: one (FM_1) acting as input and the other (FM_2) acting as output. (b) This table illustrates the basic operation of the device assuming $|V_{\mathrm{SS}}|$ to be larger than the minimum value needed for switching. These state diagrams describe the transitions of FM_1 (first bit) and FM_2 (second bit) for NOT and COPY operations. (c) Coupled spin-transport/magneto-dynamics model. Here, $\vec{I}_S$ is spin current and $\hat{m}$ is the magnetization direction.

The black regions under the magnets in Fig. 1(a) represent isolation layers in the conducting region of the channel. Such a design ensures that communication between the two magnets is limited to the channel segment between the two of them. Therefore, each magnet can interact independently with different magnets on either side. Specifically, each magnet can have a "talking" side that behaves as an input to the following stage and a "listening" side that behaves as an output to the previous stage thus allowing for cascaded ASL structures. Fig. 1(b) shows the state diagram for two interacting magnets (FM_1 and

FM_2) connected by one such channel segment and can be understood as follows.

Ordinarily, with the supply voltage $V_{SS} = 0$, the two magnets in Fig. 1(a) can exist in any of four possible states that we denote as 00, 01, 10, 11 (FM_1: first bit, FM_2: second bit). However, we will show that as V_{SS} is increased beyond a positive threshold value the only stable states are those for which the two magnets are *antiparallel*, namely 01 and 10. On the other hand, if V_{SS} is negative then beyond a certain threshold value, the only stable states are those for which the two magnets are *parallel*, namely 00 and 11. These stable states are the ones shown in Fig. 1(b) with arrows pointing back to themselves.

The key point regarding the inbuilt nonreciprocity of this device can be appreciated by considering what happens if we start from a state, say 00 that is rendered unstable when the supply voltage V_{SS} is positive and exceeds a critical value. In principle, it could make a transition to either of the two stable states 01 or 10. However, we will show that it should be possible to engineer the device so that it will transition predictably to 01 and not to 10 as indicated in Fig. 1(b). In other words, the transition arrows in the table are always "vertical" and never "horizontal," since it is always FM_2 that changes its magnetization appropriately to reach a stable state, while FM_1 never switches its magnetization.

What we wish to emphasize here is that the identical magnets FM_1 and FM_2 function like the input and the output, respectively, with an input–output isolation that is characteristic of transistors. The operation with $V_{SS} > 0$ can be viewed as a NOT operation, while the operation with $V_{SS} < 0$ can be viewed as a COPY operation.

B. Experimental Realization of ASL

In this paper, we will establish the feasibility of the above claims regarding ASL operation using a coupled spin-transport/magnetization-dynamics model [see Fig. 1(c)]. This coupled model, the details of which are given in [9], describes existing experiments such as [7] quite well. These experiments demonstrate feasibility of switching a magnet in structures similar to Fig. 1(a) with voltages of the order of a few 10 s of millivolts. Such a low-voltage operation is very attractive for switching applications. However, we would like to clearly state which features of ASL operation described earlier are experimentally established and which—at this time—are not.

First, in the present ASL structure, FM_1 and FM_2 are both identical free layers, either of which could switch as easily as the other. By contrast, all existing experiments [7], [8] utilize a free layer and a fixed layer, such that only one magnet can switch. While having a fixed layer clearly ensures "nonreciprocity," it is not suitable for logic implementation since the output of one section must subsequently function as the input to another. This requires that both the magnets should be nominally identical.

What is it then that differentiates FM_1 from FM_2 in an ASL device, making them act differently as input and output, respectively? We will discuss various possibilities in subsequent sections, such as the one shown in Fig. 2(a). Here, simply having the ground terminal closer to one of the magnets makes it function as an input as supported by our simulations in Fig. 3.

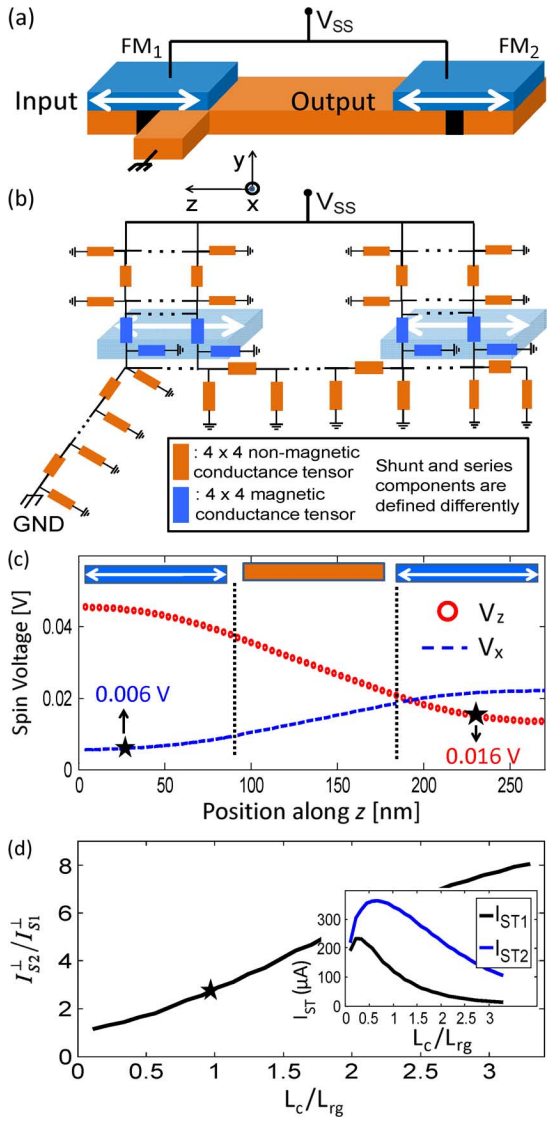

Fig. 2. Cascadable ASL design that achieves nonreciprocity through asymmetric placement of the ground terminal. (a) Position of the ground terminal is closer to the input rather than output. (Not drawn to scale.) (b) Distributed conductance network used to model the device. Each conductance element is a 4×4 tensor (see Appendix A). The shunt and series conductance elements are defined differently. (c) z and x components of spin voltage in the channel region assuming input magnet is along z and output magnet is along x. A higher spin voltage underneath the output magnet as compared to the input magnet results in higher spin torque current getting exerted on output as compared to input. (d) Ratio of torques exerted on FM_1 (input) and FM_2 (output) magnets as a function of contact length normalized to the "rg" length.

Second is the application of the same supply voltage V_{SS} to both the input and output magnets, which is attractive from a practical point of view, since it is easier to apply the same voltage to closely spaced structures, and, also minimizes the associated capacitive charges. Normally, if we wish one magnet to turn another, it may not seem natural to apply the same voltage to the two magnets. Indeed, the experiment in [7] had the output magnet left floating as is common with nonlocal spin valve experiments [13]. However, it will be shown later that the stability of the final states, i.e., FM_1 and FM_2 being parallel or antiparallel to each other is a feature peculiar to having the same supply voltage on both magnets. Additionally, it will also be shown in Appendix B that the operational regime with different supply

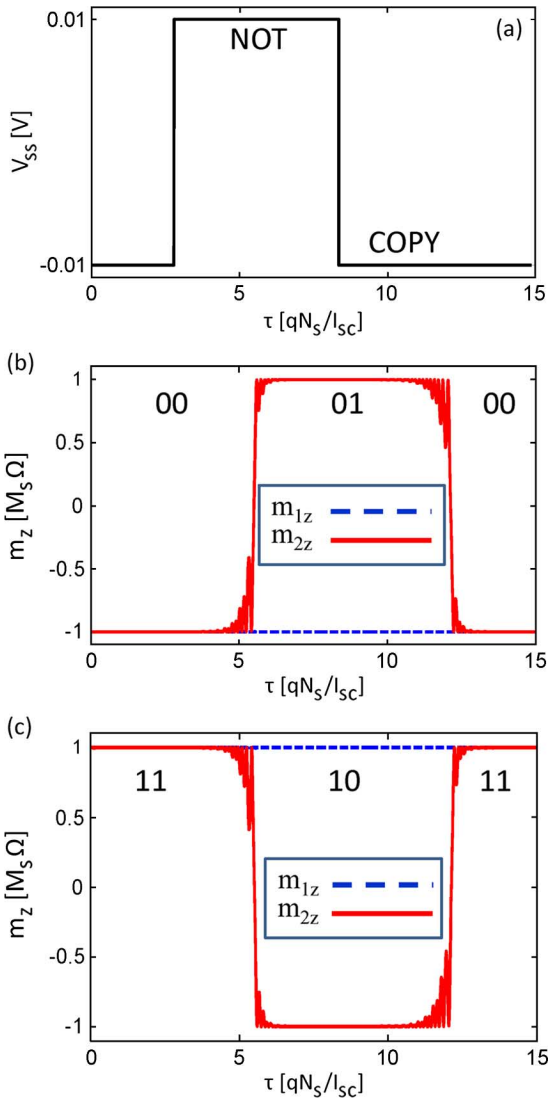

Fig. 3. Coupled spin-transport/LLG simulations describing the NOT and COPY operations in an ASL device with inbuilt nonreciprocity. (a) Voltage pulse applied to the structure of Fig. 2(a). (b) Both magnets are initialized at 00. With $V_{\rm SS} < 0$, the parallel states are stable and 00 state is retained. But when the voltage is changed to $V_{\rm SS} > 0$, the output becomes the NOT of input and antiparallel state (01) is reached which is now stable. System reaches 00 again when voltage is changed back to positive values and is stable again. (c) Similar simulations as in part (b) but with the two magnets initialized at 11 state.

voltages to the input and output magnets has its own interesting characteristics that could have potential applications.

C. Outline

As discussed earlier the key features distinguishing ASL operation [see Fig. 1(b)] are as follows.

1) Its transition diagram allows only "vertical transitions" dictated by the input magnet.
2) *Stable states (01, 10 for $V_{SS} > 0$ and 00, 11 for $V_{SS} < 0$).*

These two features are first established in Section II through detailed numerical simulations. Next, Section III provides an intuitive understanding of the ASL state diagram.

In Section IV, we show that ASL devices [each identical to the one in Fig. 2(a)] with inbuilt directionality can be cascaded to construct circuits. Our simulations suggest that three identical nanomagnets (see Fig. 5) linked by spin transport channels can form a chain of inverters with a directed transfer of information (magnetization) from one magnet to the next: $1 \rightarrow 2 \rightarrow 3$. This inbuilt directivity also allows the last magnet in the chain to drive the first one, when connected, to function like a classic ring oscillator (see Fig. 6) well known in CMOS circuits.

II. Establishing the ASL State Diagram

In this section, we will present numerical evidence supporting the state diagram in Fig. 1(b) using an experimentally benchmarked model [9]. Fig. 2(a) shows one implementable scheme for introducing nonreciprocity in the ASL device. The difference from Fig. 1(a) is that here the lead to ground is shifted to the channel region lying below $\rm FM_1$ thus making it the input. $\rm FM_1$ effectively shields $\rm FM_2$ from communicating with the ground terminal, thereby reducing the charge current and consequently the spin current $\vec{I}_S$ injected by $\rm FM_2$ as compared to $\rm FM_1$. As a result, the torque exerted on $\rm FM_2$ given by $\vec{I}_S^{\perp} = \hat{m}_2 \times (\vec{I}_{S2} \times \hat{m}_2)$ is greater than the torque exerted on $\rm FM_1$. This effect is captured by the distributed version [see Fig. 2(b)] of the conductance model for spin transport introduced in [9] which accounts for the spatial variation of quasi-Fermi levels in the channel for charge as well as each spin component. We use the same parameters as in the experiment [7] to present our results for identical magnets. As an illustrative example, Fig. 2(c) and (d) shows the numerical results for the specific case when $\rm FM_1$ is along $\hat{z}$ and $\rm FM_2$ is along $\hat{x}$. Fig. 2(c) shows how a higher injection by $\rm FM_1$ results in a larger $\hat{z}$ spin voltage distribution in the vicinity of $\rm FM_2$ compared to the $\hat{x}$ spin voltage in the vicinity of $\rm FM_1$. The ability of the input magnet to shield the output magnet from the ground terminal depends on the ratio of the magnet contact length L_C to the transfer length of the contact which is of the order: $L_{rg} = 1/\sqrt{r\rho/WA}$, where $g =$ contact conductance, $W =$ width of the channel, $\rho =$ channel resistivity, and $A =$ cross-sectional area of the channel. The ratio of spin-torques $I_{S2}^{\perp}/I_{S1}^{\perp}$ follows from V_Z/V_X as is evident by comparing Fig. 2(c) and (d). Fig. 2(c) was simulated for the particular case of $L_C \sim L_{rg}$ and the corresponding point can be identified in Fig. 2(d).

Fig. 3 shows a typical simulation result for such a structure from our coupled model [see Fig. 1(c)] of spin-transport and dynamics of magnetization $\hat{m}$ described by the Landau–Lifshitz–Gilbert (LLG) equation:

$$\frac{d\hat{m}}{dt} = -|\gamma|\hat{m} \times \vec{H}_{\rm int} + \alpha\hat{m} \times \frac{d\hat{m}}{dt} + \frac{\vec{I}_s^{\perp}}{qN_s} \qquad (1)$$

where γ is the gyromagnetic ratio, α is the Gilbert damping coefficient, q is the charge of an electron. N_s is the net number of Bohr magnetons in a nanomagnet given by $N_S = M_S\Omega/\mu_B$ (M_s: saturation magnetization, Ω: volume, and μ_B: Bohr magneton). $\vec{H}_{\rm int}$ describes the internal fields of a magnet. Note that each magnet is described simultaneously by its independent LLG equation.

The solid curves in Fig. 3(b) and (c) show the state of the output magnet and the dashed curves show the state of the input magnet as a function of the dimensionless time τ in units of qN_S/I_{SC}. I_{sc} is the critical spin-current [10] needed for switching given by

$$I_{sc} = \frac{2q}{\hbar}(2\alpha E_b)(1 + H_d/2H_K)$$

where $\hbar$ is the reduced Plank's constant, E_b is the anisotropy energy barrier, H_d is the demagnetizing field, and H_K is the uniaxial anisotropy field. Note that the absence of H_d in perpendicular magnetic anisotropy magnets [18] would reduce the critical spin current. Such issues are discussed in [9].

These figures show that when $V_{SS} < 0$, the initial parallel states (00 and 11) are retained and are stable. Once $V_{SS} > 0$, the output becomes the NOT of the input resulting in antiparallel states (01 and 10) which under positive voltages are stable states. As V_{SS} is changed back to negative values, the output once again becomes the copy of the input and the resulting parallel states are stable. Our coupled model effectively establishes the state diagram in Fig. 1(b).

III. "Understanding" the State Diagram

Now that we have presented numerical evidence supporting the transition diagram [see Fig. 1(b)]; let us try to understand the underlying physics.

A. How the Stable States are Determined?

As indicated in Fig. 1(b), with a negative voltage V_{SS}, the parallel states 00 and 11 are stable, while with a positive V_{SS}, the antiparallel states 01 and 10 are the stable ones. To understand this, we first note that, in general, the spin-currents entering the two magnets can be written as [17]

$$\vec{I}_{s1} = A_1\hat{m}_1 + B_1\hat{m}_2 + C_1(\hat{m}_1 \times \hat{m}_2) \quad (2a)$$

$$\vec{I}_{s2} = A_2\hat{m}_2 + B_2\hat{m}_1 + C_2(\hat{m}_2 \times \hat{m}_1) \quad (2b)$$

so that the spin-torques (s.t.) due to these spin-currents can be written as (Note: $c \equiv \hat{m}_1.\hat{m}_2$)

$$qN_s\frac{d\hat{m}_1}{dt}\bigg|_{s.t.} = \vec{I}_{s1} - (\vec{I}_{s1}\cdot\hat{m}_1)\hat{m}_1 = -cB_1\hat{m}_1 + B_1\hat{m}_2 + C_1(\hat{m}_1\times\hat{m}_2) \quad (3a)$$

$$qN_s\frac{d\hat{m}_2}{dt}\bigg|_{s.t.} = \vec{I}_{s2} - (\vec{I}_{s2}\cdot\hat{m}_2)\hat{m}_2 = -cB_2\hat{m}_2 + B_2\hat{m}_1 + C_2(\hat{m}_2\times\hat{m}_1). \quad (3b)$$

These spin-torque currents are only a part of the terms that enter the right-hand side of the LLG equation. But suppose we ignore the other terms involving the internal fields and use (3a) and (3b) to write

$$\Rightarrow \frac{d}{dt}c = \frac{d\hat{m}_1}{dt}.\hat{m}_2 + \frac{d\hat{m}_2}{dt}.\hat{m}_1 = (B_1 + B_2)(1 - c^2). \quad (4)$$

Although this equation does not include the effective internal fields, it does seem to explain the stable states correctly.

Clearly from (4), the fixed points where $dc/dt = 0$, are given by $1 - c^2 = 0$, i.e., $c = +1$ (parallel magnets) and $c = -1$ (antiparallel magnets). Of these two, however, only one is stable, the one for which $(B_1 + B_2)c > 0$, so that the "Jacobian" for (4) is negative.

For a positive $(B_1 + B_2)$, this means that the stable configuration is $c = +1$ corresponding to parallel, while for negative $(B_1 + B_2)$, the stable configuration is $c = -1$ corresponding to antiparallel. This would explain the stable states in Fig. 1(b), if the sign of $(B_1 + B_2)$ is opposite to that of V_{SS}. This is indeed true and can be understood as follows. A negative V_{SS} applied to a ferromagnet results in the channel being populated preferentially by spins in the direction of the injecting ferromagnet [15] giving a positive value for B, while a positive V_{SS} populates the channel preferentially with spins in the direction opposite to the ferromagnet, resulting in a negative value for B.

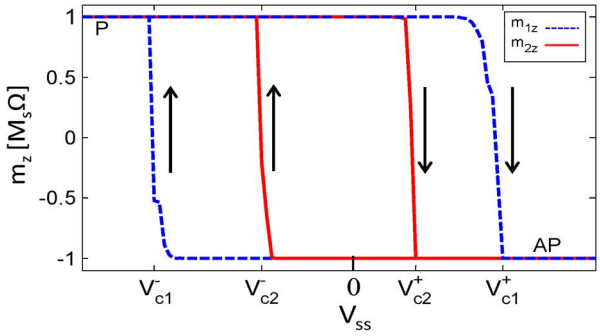

Fig. 4. Different switching voltages for *identical* input and output magnets. The antiparallel (AP) states are stable for positive V_{SS} while parallel (P) states are stable for negative V_{SS}. FM_1 and FM_2 differ only in the placement of the ground lead as illustrated in Section II.

B. Why Transitions are Vertical?

It can be shown that initially even if both magnets start to switch in Fig. 3(b) and (c), the output magnet gets going faster and soon the input magnet goes back to its initial state, since the overall objective of both magnets is the same: they both want to be antiparallel for $V_{SS} > 0$, and parallel for $V_{SS} < 0$.

Why does one magnet get going faster? Essentially because the other magnet being closer to the ground terminal is more efficient in generating the spin currents needed to switch it. This difference can be quantified by considering a Gedanken experiment. Suppose using the device in Fig. 2(a), we first hold FM_1 fixed and only allow FM_2 to switch. At low voltages, the spin current injected by FM_1 does not provide sufficient torque to affect FM_2. As the voltage is ramped up (see Fig. 4), FM_2 gets switched at some voltage V_{c2}^+. Next, suppose the experiment is reversed: FM_2 is held fixed and FM_1 is allowed to switch which occurs at a different critical voltage V_{c1}^+. Similar experiments can be repeated for $V_{SS} < 0$ to obtain the corresponding critical voltages. For a perfectly symmetric ASL, $V_{c1}^+ = V_{c2}^+$. The difference between V_{c1} and V_{c2} arises from any asymmetry, intentional or unintentional, in the structure.

For example, Fig. 4 was generated for the situation where FM_1 and FM_2 differ only in the placement of the ground lead as illustrated in Section II. This asymmetry dictates that a higher voltage is required to generate enough spin current to switch FM_1. In essence, the window $V_{c1} - V_{c2}$ is a direct measure of the nonreciprocity in the system.

V_{c1} and V_{c2} delineate the range of supply voltages into three distinct regimes. When $|V_{SS}| < V_{c2}$, no magnet has enough spin current to switch. So, all four states 00, 10, 11, and 01 are stable. As the voltage is further increased $V_{c2} < |V_{SS}| < V_{c1}$, only FM_2 has enough current to switch and the magnets finally stabilize in antiparallel (parallel) for positive (negative) V_{SS}. The stability in this regime is expected since the operation is in a window where only one magnet can switch.

When $V_{c2} < V_{c1} < |V_{SS}|$, there is sufficient torque acting on both FM_1 and FM_2 to switch either of them. However, it is seen

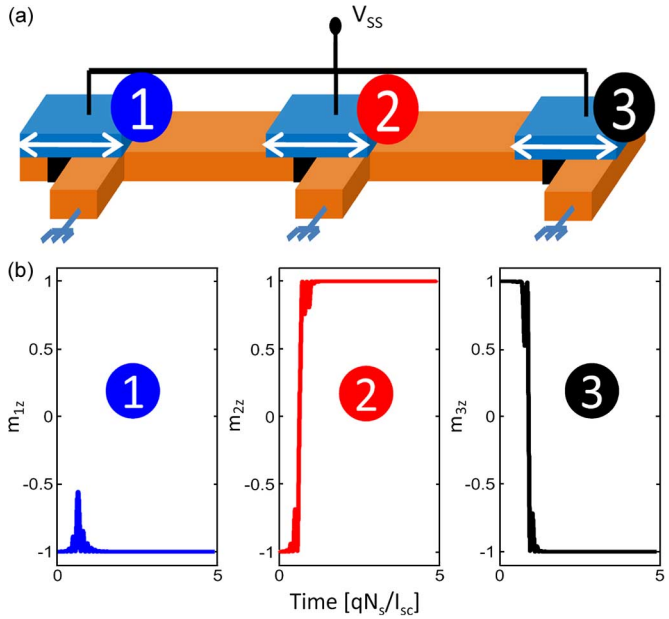

Fig. 5. Chain of inverters showing the cascading of ASL devices. (b) Three-magnet system is initialized at 001. At time $t = 0$, the voltage is turned ON. Once the steady state is reached, the final state of the three-magnet system becomes 010. Since directivity is present, magnet 1 dictates the state of magnet 2 and that in turn decides the state of magnet 3.

that it is only FM_2 that switches. The reason is that the induced asymmetry ensures that the torques on FM_2 is greater than the torque on FM_1 and the time that they would have taken to switch is different. Initially, both magnets start to switch. However, as soon as FM_2 switches, FM_1 relaxes to its original state which is the stable state of the two magnet system as discussed earlier. In the absence of any asymmetry, the switching behavior is not predictable. In reality, however, an asymmetry will ensure which magnet will predictably switch and the challenge is to deliberately engineer an asymmetry large enough to overcome random variations and enforce the desired switching behavior. We will discuss additional schemes for engineering such asymmetry in the Appendix.

IV. Cascading ASL Devices

Having established numerically as well as provided simple analytical reasoning in previous sections, the validity of ASL operation given in Fig. 1(b), we now show that multiple ASL devices with inbuilt directionality [such as in Fig. 2(a)] can be cascaded to construct circuits [16].

Let us first consider the simple example of three identical magnets connected in series as shown in Fig. 5. When a positive voltage is applied to this circuit, each magnet tries to invert the ones connected to it. However, the placement of the ground lead enforces a directed transfer of information (magnetization) in a specific order: $1 \rightarrow 2 \rightarrow 3$. Consequently, the circuit behaves as a chain of inverters. This is illustrated in Fig. 5(b) where initially both FM_1 as well as FM_2 start to switch. However, FM_1 dominates and it is FM_2 that gets inverted from logic "0" to "1." Subsequently, FM_2 inverts FM_3 and the system becomes stable.

It is important to note that such directed transfer of information could be attempted using either nonidentical magnets (such as making them progressively smaller) or using additional

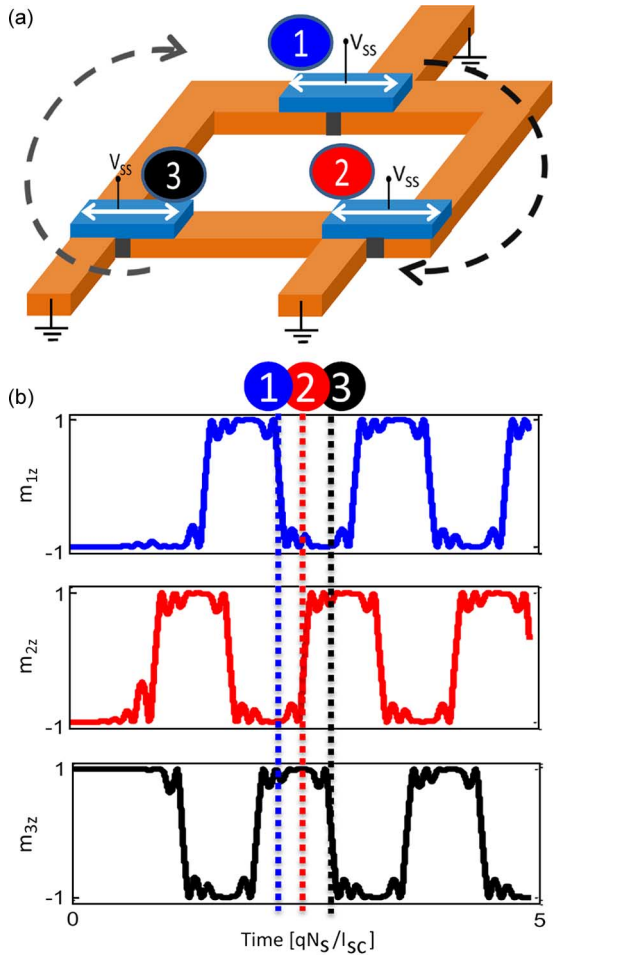

Fig. 6. (a) Ring oscillator composed of three identical magnets in cascaded ASL devices. (b) This system will oscillate with a positive dc supply voltage applied to the magnets. The direction of information flow is $1 \rightarrow 2 \rightarrow 3$. The process continues in a cyclic fashion. The switching edges—identified by the vertical dashed lines—for magnets 1, 2, and 3 show the step by step process of information transfer from one magnet to the next.

clocking circuitry. However, additional clocking would introduce its own design complexity and power dissipation issues. Similarly, using nonidentical magnets is not feasible in the context of integrated circuits with many devices. Also, from an operational point of view the "small" last magnet of the chain would not be able to drive earlier stages thus preventing information transfer in a loop.

The power of inbuilt directivity using identical magnets is clearly illustrated by the example of a classic ring oscillator (see Fig. 6) well known in CMOS circuits. It allows sufficient feedback from the last magnet in the chain of identical magnets to drive the first one without any clocking circuitry.

V. Concluding Remarks

Electronic devices have traditionally been based on controlling the flow of charge. However, electrons carry both charge and "spin," the latter being responsible for magnetic phenomena. In the last ten years, there have been significant advances in our ability to control the spin current in electronic devices and their interactions with nanomagnets. A recent proposal for ASL proposes to store information in nanomagnets which communicate using spin currents for communication.

ASL is defined by: *Information*: magnetization of magnet, *Communication*: spin current, *Energy*: power supply. This is similar to the charging of an output capacitor according to the information provided by the charge on an input capacitor in standard CMOS logic: *Information*: charge on capacitor, *Communication*: charge current, *Energy*: power supply.

However, a key element in any approach for logic implementation is the input–output isolation that comes so easily in transistors that it often goes unnoticed. The purpose of this paper is to present a unique approach of achieving nonreciprocal operation with ASL devices based on spin-torque physics that could enable combinational logic similar to CMOS. Using a model for ASL devices that is based on established physics and is benchmarked against available experimental data, we present interesting predictions that we hope will inspire creative experimentation along these lines. The ring oscillator and chain of inverters shown in this paper are just two demonstrative examples of all-spin computation. The principles put forth in this paper can be used to build more complex circuits which we leave as future work.

APPENDIX

A. Other Schemes for Nonreciprocity With Common Vss

The ASL state diagram [see Fig. 1(b)] was established earlier using asymmetric ground layout. However, this could have been achieved through other structural asymmetries. To investigate other possibilities, let us first quantify the nonreciprocity. The degree of nonreciprocity can be arrived at by defining a "spin-torque conductance" relating the spin-torque component of the current at each of the magnets in the ASL device to the externally applied voltage:

$$\left|\vec{I}_{s1}^{\perp}\right| \equiv \left|\hat{m}_1 \times \left(\vec{I}_{s1} \times \hat{m}_1\right)\right| = g_{s1} V_{SS}$$
$$\left|\vec{I}_{s2}^{\perp}\right| \equiv \left|\hat{m}_2 \times \left(\vec{I}_{s2} \times \hat{m}_2\right)\right| = g_{s2} V_{SS}.$$

The magnet with the larger magnitude of g_s functions as the output.

Fig. A1 shows the simplest conductance model to analyze the ASL structure [see Fig. 1(a)] with the ground lead now in the center of the channel. This model allows us to obtain an exact analytical expression that matches the distributed numerical model in Fig. 2(b) for near-ballistic channels.

Note that each of the conductances is a 4×4 matrix and relates 4×1 voltages and currents that include charge (c), and the three (x, y, z) spin components, i.e., $[\mathrm{c, z, x, y}]^{\mathrm{T}}$.

For a Ferromagnet in the "z-"direction, the interface conductances are given by G_F and G_{0F} as follows:

$$G_F = \begin{pmatrix} g_F & g_\alpha & 0 & 0 \\ g_\alpha & g_F & 0 & 0 \\ 0 & 0 & 0 & 0 \\ 0 & 0 & 0 & 0 \end{pmatrix}, \quad G_{0F} = \begin{pmatrix} 0 & 0 & 0 & 0 \\ 0 & 0 & 0 & 0 \\ 0 & 0 & g_\beta & -g_\gamma \\ 0 & 0 & g_\gamma & g_\beta \end{pmatrix}$$

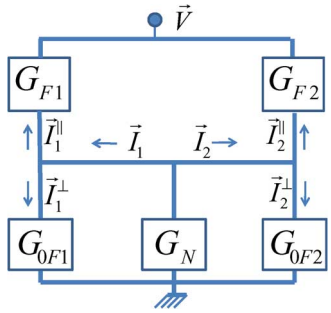

Fig. A1. Circuit representation of an ASL device for a one-point channel that is used to derive a relatively simple closed form equation (A1) describing devices with near ballistic channels. [Note that the simulations use a distributed conductance network as illustrated in Fig. 2(b).]

where g_F is the conductance of the FM/interface region, $g_\alpha = Pg_F$, and P is the effective polarization of the FM interface. g_β and g_γ refer to the effective spin "mixing" conductance of the interface as defined in [11] and describe the Slonczewski and field-like components of spin torque, respectively. In the subsequent analysis, we set $g_\gamma = 0$ because in general the field-like term is found to be very small in all-metallic structures [14]. We assume the lead to the ground terminal to be unpolarized with the absence of any spin-orbit interaction effects, thereby, equally affecting all spin components. It can be described by a matrix (see [9] and [12], [13] therein)

$$G_N = \begin{pmatrix} g_0 & 0 & 0 & 0 \\ 0 & g_{0P} & 0 & 0 \\ 0 & 0 & g_{0P} & 0 \\ 0 & 0 & 0 & g_{0P} \end{pmatrix}$$
$$\text{where } g_0 = \frac{A}{\rho L};\ g_{0P} = \frac{A}{\rho\lambda}\coth\left(\frac{L}{\lambda}\right)$$

ρ, λ, L, and A refer to the resistivity, spin-diffusion length, length, and cross section of the lead, respectively.

Solving the conductance model in Fig. A1 gives us an expression for the degree of nonreciprocity given by (A1). (See equation at the bottom of the page.) It is instructive to look at a simplified version of (6) for two perpendicular magnets ($\theta = \pi/2$), for which the expression simplifies to

$$\frac{|g_{S2}|}{|g_{S1}|} = \frac{g_{\alpha 1} g_{\beta 2}(g_{\beta 1} + g_{0P} + g_{F2})}{g_{\alpha 2} g_{\beta 1}(g_{\beta 2} + g_{0P} + g_{F1})}. \tag{A2}$$

Equation (A2) suggests several possibilities for implementing nonreciprocity in a controlled way by engineering the various components of the device structure. Among other things, the nonreciprocity depends on how well the input magnet can inject polarized spin current $g_{\alpha 1}$ and how easily the output magnet can relax the noncollinear spins $g_{\beta 2}$ and *vice versa*.

Different schemes for introducing nonreciprocity include: 1) insertion of a tunnel barrier at the interface of one side of the

$$\frac{g_{s2}}{g_{s1}} \equiv \frac{\left|I_{S2}^{\perp}\right|}{\left|I_{S1}^{\perp}\right|} = \left(\frac{g_{\beta 2}}{g_{\beta 1}}\right) \frac{\left(2g_{\alpha 2}\cos^2\frac{\theta}{2}\right)(g_{\beta 1} - g_{F1}) + g_{\alpha 1}(g_{0P} + g_{F2}) + g_{\alpha 2} g_{F1} + (g_{\alpha 1} - g_{\alpha 2}) g_{\beta 1}}{\left(2g_{\alpha 1}\cos^2\frac{\theta}{2}\right)(g_{\beta 2} - g_{F2}) + g_{\alpha 2}(g_{0P} + g_{F1}) + g_{\alpha 1} g_{F2} + (g_{\alpha 2} - g_{\alpha 1}) g_{\beta 2}}. \tag{A1}$$

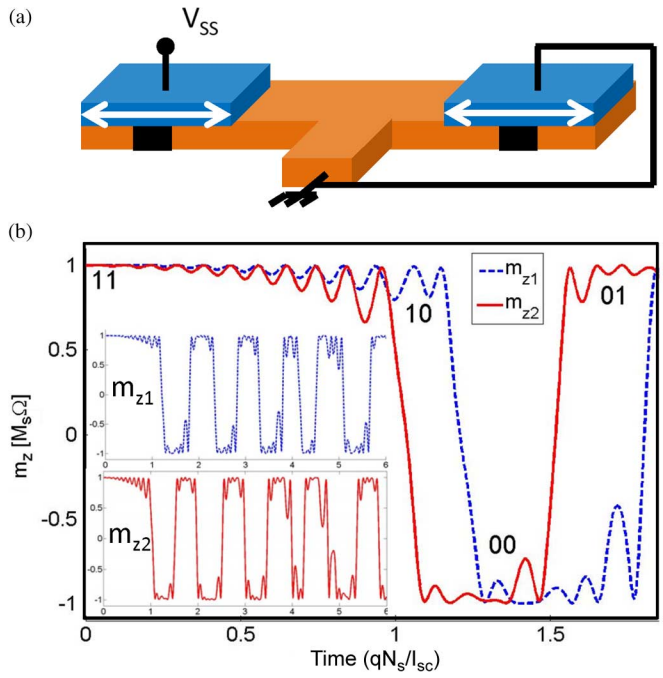

Fig. A2. Structurally symmetric ASL device with nonreciprocity induced by two different voltages applied to the input and output magnets. (a) Output magnet shorted to ground. (b) Evolution of the two magnets in this case with application of $V_{SS} > 0$. (Inset) Magnets make astable periodic oscillations.

magnets; 2) defining different interface areas for the input and output; and 3) novel techniques for designing different injection efficiencies at the input and output magnet. Such schemes could involve simultaneously altering the effective polarization as well as resistance of the interface and these effects would all be captured by (A1). These different schemes all need to be explored carefully. Our purpose here is simply to identify the relevant parameters, using a simple static analysis based on the spin-circuit model.

B. Nonreciprocity Using Different Voltages

It is also possible to introduce nonreciprocity in a physically symmetric structure simply through applying different voltages at the two magnets. We show one such case in Fig. A2(a) where one of the magnets is connected to *V*ss and the other is grounded.

The nonreciprocity in this case is given by

$$\frac{|g_{S2}|}{|g_{S1}|} = 1 + \frac{\frac{g_0}{g_F}}{1 - \frac{2g_\alpha^2 \cos^2 \frac{\theta}{2}}{g_F(g_F + g_{0P} + g_\beta)}}.$$

In general, the magnet with a supply voltage closer to that of the ground terminal ends up with a higher value of g_S. However, this system has no stable state and once the output has switched, the system continues to oscillate deterministically between all the states 00, 01, 11, and 10. The oscillations are primarily due to the fact that magnets try to enforce opposite configurations as one of them is injecting spins while the other is extracting spins. While these oscillations make it difficult to implement logic in this configuration, the periodic astable oscillations might have their interesting (see Fig. A2(b) insets) applications.

ACKNOWLEDGMENT

This work was supported by the Institute for Nanoelectronics Discovery and Exploration under the Nanoelectronics Research Initiative program as well as National Science Foundation Center for Science of Information. The authors are grateful to J. Appenzeller and and S. Salahuddin for insightful discussions on possible experimental layouts. S. Srinivasan also thanks K. Y. Camsari for helpful discussions.

REFERENCES

[1] T. N. Theis and P. M. Solomon, "It's time to reinvent the transistor!," *Science*, vol. 327, no. 5973, pp. 1600–1601, Mar. 2010.
[2] A. Imre, G. Csaba, L. Ji, A. Orlove, G. H. Bernstein, and W. Porod, "Majority logic gate for magnetic quantum-dot cellular automata," *Science*, vol. 311, pp. 205–208, Jan. 2006.
[3] D. B. Carlton, N. C. Emley, E. Tuchfeld, and J. Bokor, "Simulation of nanomagnet-based logic architecture," *Nano Lett.*, vol. 8, no. 12, pp. 4173–4178, Nov. 2008.
[4] B. Behin-Aein, D. Datta, S. Salahuddin, and S. Datta, "Proposal for an all-spin logic device with built-in memory," *Nature Nanotech*, vol. 5, pp. 266–270, Feb. 2010.
[5] G. Csaba, W. Porod, and A. Csurgay, "A computing architecture composed of field-coupled single domain nanomagnets clocked by magnetic field," *Int. J. Circuit Theory Appl.*, pp. 67–82, Jan./Feb. 2003.
[6] J. Atulasimha and S. Bandyopadhyay, "Bennett clocking of nanomagnetic logic using multiferroic single-domain nanomagnets," *Appl. Phys. Lett.*, vol. 97, p. 173105, Oct. 2010.
[7] T. Yang, K. Kimura, and Y. Otani, "Giant spin accumulation and pure spin-current-induced reversible magnetization switching," *Nature Phys.*, vol. 4, pp. 851–854, Oct. 2008.
[8] J. Z. Sun, M. C. Gaidis, E. J. O'Sullivan, E. A. Joseph, G. Hu, D. W. Abraham, J. J. Nowak, P. L. Trouilloud, Y. Lu, S. L. Brown, D. C. Worledge, and W. J. Gallagher, "A three-terminal spin-torque-driven magnetic switch," *App. Phys. Lett.*, vol. 95, p. 083506, Aug. 2009.
[9] B. Behin-Aein, A. Sarkar, S. Srinivasan, and S. Datta, "Switching energy-delay of all-spin logic devices," *App. Phys. Lett.*, vol. 98, p. 123510, 2011.
[10] J. Z. Sun, "Spin-current interaction with a monodomain magnetic body: A model study," *Phys. Rev. B*, vol. 62, pp. 570–578, Jul. 2000.
[11] A. Brataas, G. E. W. Bauer, and P. J. Kelly, "Non-collinear magnetoelectronics," *Phys. Rep.*, vol. 427, pp. 157–255, Apr. 2006.
[12] T. Valet and A. Fert, "Theory of perpendicular magnetoresistance in magnetic multilayers," *Phys. Rev. B*, vol. 48, pp. 7099–7113, Sep. 1993.
[13] M. Johnson and R. H. Silsbee, "Thermodynamic analysis of interfacial transport and of the thermomagnetoelecric system," *Phys. Rev. B*, vol. 35, pp. 4959–4972, Apr. 1987.
[14] K. Xia, P. J. Kelly, G. E. W. Bauer, A. Brataas, and I. Turek, "Spin torques in ferromagnetic/normal-metal structures," *Phys. Rev. B*, vol. 65, p. 220401(R), May 2002.
[15] F. Casanova, A. Sharoni, M. Erekhinsky, and I. K. Schuller, "Control of spin injection by direct current in lateral spin valves," *Phys. Rev. B*, vol. 79, p. 184415, May 2009.
[16] S. Srinivasan, A. Sarkar, B. Behin-Aein, and S. Datta, "Unidirectional information transfer with cascaded all spin logic devices," in *Proc. Annu. Dev. Res. Conf.*, 2011.
[17] A. Brataas and G. Bauer, "Non-collinear magnetoelectronics," *Phys. Rep.*, vol. 427, no. 4, pp. 157–255, 2006.
[18] H. Meng and J. P. Wang, "Spin transfer in nanomagnetic devices with perpendicular anisotropy," *App. Phys. Lett.*, vol. 88, p. 172506, 2006.